https://doi.org/10.5194/egusphere-2023-2823
Preprint. Discussion started: 12 February 2024

Local ship speed reduction effect on black carbon emissions measured at remote marine station

Mikko Heikkilä[1], Krista Luoma[1], Timo Mäkelä[1], and Tiia Grönholm[1]

[1]Finnish Meteorological Institute, Helsinki, Finland

Correspondence: Mikko Heikkilä (mikko.heikkila@fmi.fi)

Abstract. Speed restrictions for ships have been introduced locally to reduce the waves and turbulence causing erosion, and safety hazards, and to mitigate the air and underwater noise emissions. Ship speed restrictions could be used to minimise the climate impact of maritime transport since many air pollutants in ship exhaust gas are reduced when travelling at lower speeds. However, for example, methane and black carbon emissions do not linearly correlate with the load of internal combustion engines. Therefore, the effect of speed restrictions may not be trivial. Black carbon concentrations from ship plumes were examined at the remote marine site in the Finnish Southwestern archipelago. Ships with service speeds over 15 knots and equipped with an exhaust gas cleaning system were analysed for black carbon emissions as a function of speed. Both unadjusted and weather-adjusted main engine loads were modelled to determine load-based emission factors. Black carbon concentration per kilogram of fuel decreased as a function of engine load. However, as calculated per hour the black carbon emission increased as a function of ship speed except around a constant emission area, which was roughly 15-20 knots. In terms of local air quality, total black carbon emission per nautical mile was the highest around the halved speeds, 10-13 knots, or when the speed was higher than 20-23 knots. From a climate warming perspective, the CO_2 emissions dominated the exhaust gas and reducing the speed decreased the global warming potential in CO_2 equivalent both per hour and per nautical mile.

1 Introduction

Speed limits have been discussed widely as a measure to mitigate the effects of underwater noise, air, and water pollution originating from seagoing vessels (e.g. MacGillivray et al., 2019; Woo and Im, 2022). As the resistance of the vessel moving through the water is known to be the largest contributing factor for fuel consumption (Hollenbach, 1998), it is then natural to assume that restricting speeds would directly lead to a reduction in air emissions (Yau et al., 2012). However, the problem is not simple: restricting speed could lead to an increase in the need for carriage and therefore, to an increase in total emissions (Elkafas and Shouman, 2021; Tan et al., 2022). Local speed limits have been introduced in many areas for a variety of reasons. Safety is one of the primary concerns. Also, erosion is increased when ships operate at higher speeds causing wake and turbulence (Almström et al., 2021, 2022; Almström and Larson, 2020; Benassai et al., 2013; Bilkovic et al., 2019; Dam et al., 2008; Roo and Troch, 2015; Gunnel et al., 2014; Houser, 2010; Parnell et al., 2015; Stumbo et al., 1999). Recently, also underwater noise has become a relevant factor when considering vessel speeds (Jalkanen et al., 2022; Lajaunie et al., 2023).

https://doi.org/10.5194/egusphere-2023-2823
Preprint. Discussion started: 12 February 2024

Air emissions from ships can be categorised roughly by their impact on global warming and air quality. In many cases, focusing only on one could have a negative impact on the other. California has successfully implemented voluntary speed limits in the effort of mitigating air pollution from sea-going vessels (Linder, 2018), as many pollutants such as nitrogen oxides (NO_x) and particulate matter (PM) are associated with detrimental health and environmental effects (Chen and Hoek, 2020; Nunes et al., 2020; Orellano et al., 2020; Viana et al., 2020; Wang et al., 2020, 2019; Zhang et al., 2021).

Black carbon (BC) emissions from marine engines have been studied widely using various methods to establish accurate emission factors ($g\,BC\,(kg\,fuel)^{-1}$) for different engine and vessel types (e.g., Cappa et al., 2014; Corbin et al., 2020; Lack et al., 2008; Schlaerth et al., 2021) and the association between engine load and BC emissions has been shown (Jiang et al., 2018; Lack and Corbett, 2012). The Intergovernmental Panel on Climate Change (IPCC) report in 2007 noted that the effect of BC on climate change is probably larger than previously thought (Service, 2008), and recently, associations have been made also between health effects and BC from ships (Lepistö et al., 2022).

Monitoring and inventorying ship emissions have traditionally been done by bottom-up modelling using ship Automatic Identification System (AIS) data combined with emission factors (e.g. Jalkanen et al., 2009, 2012; Woo and Im, 2021) and very recently also combining meteorological factors in the resistance modelling (Kim et al., 2023). Establishing accurate emission factors and modelling the contribution of weather impact relies on model-testing, remote sensing and measurements conducted in both test-bed conditions and onboard. There still lies a knowledge gap between what is known and what is unknown, especially concerning ships equipped with exhaust gas cleaning systems (EGCS) that are getting more popular since the global reduction of ship fuel sulphur content in 2020. This research aims to answer the question of what is the local effect of restricting speed to ship BC emissions and how aerodynamic resistance caused by wind and the hydrodynamic effect of waves impact modelling the correct main engine load on a ship.

2 Data and methods

2.1 Measurement site

Exhaust gas plumes originating from passing ships between 26th May 2022 - 14th October 2023 were examined at the remote sensing site of Utö island (59° 47'N 021° 22'E) situated at the outermost part of the Finnish South-West archipelago (Figure 1). The island is small, its area is 0.81 km^2 and its year-round population is less than 40 people. Ships entering and exiting the ports of cities Turku and Naantali pass in proximity (approximately 500 meters) of the Utö island. Moreover, in Utö there is a pilot station to supply pilotage for the archipelago fairway. Pilot boarding speed is normally around 10 knots, which means that vessels with higher operating speeds need to slow down significantly for the pilot boarding or disembarking, and ships that have service speeds close to the boarding speed do not need to alter speed. Some of the passing vessels are on regular routes to and from the ports supplied by the Utö fairway and their officers carry pilot exemptions. In this case, these ships do not need to slow down at the pilot station. Based on this a dataset was created with as many ships as possible passing the pilot station at various speeds.

https://doi.org/10.5194/egusphere-2023-2823
Preprint. Discussion started: 12 February 2024

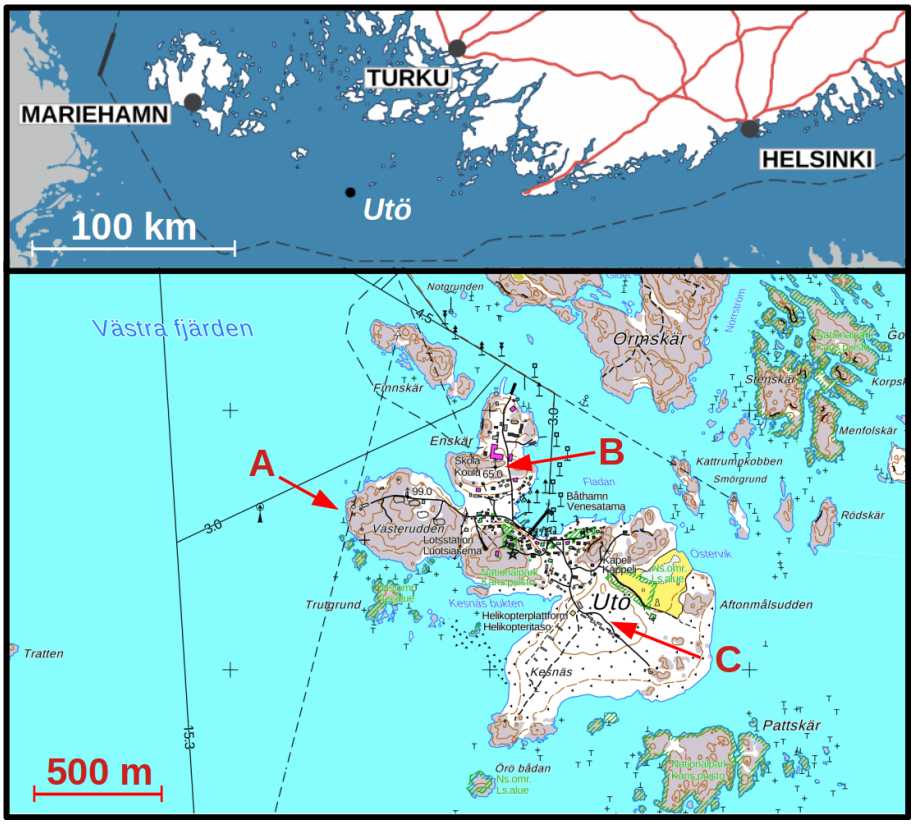

Figure 1. Utö location at Finnish south-west archipelago and below a detailed map of Utö island. Measurement locations are shown in the map by three red arrows A) Sea station, B) ICOS-station, and C) Air quality station. Black thin lines present the center of the shipping fairways. The fairway in the north-west direction on the western side of the island is the main shipping lane in the area. The maximum draught of the fairway for safe navigation is 15.3 m

A wide range of meteorological, aerosol particle, gas, and biological measurements are carried out in Utö Atmospheric and Marine Research Station owned by Finnish Meteorological Institute (FMI) (Laakso et al., 2018). The station belongs, for example, to the HELCOM marine monitoring network and to the Integrated Carbon Observation System ICOS. The station has three different measurement locations A) Sea station, B) ICOS-station, and C) Air quality station (see the map of Utö, Fig. 1).

2.2 Ship position data and plume identification

An AIS receiver and an automatic camera are installed in the Sea station. When the AIS signal from the approaching ship is received, the camera starts automatically to take pictures every 30 seconds. Meteorological data (wind velocity and direction, pressure, and temperature) are measured in the Sea station and synchronized with the AIS data in the file. The plumes were identified manually by checking the AIS information of bypassing ships and possible increases in the BC and CO_2 when the

https://doi.org/10.5194/egusphere-2023-2823
Preprint. Discussion started: 12 February 2024

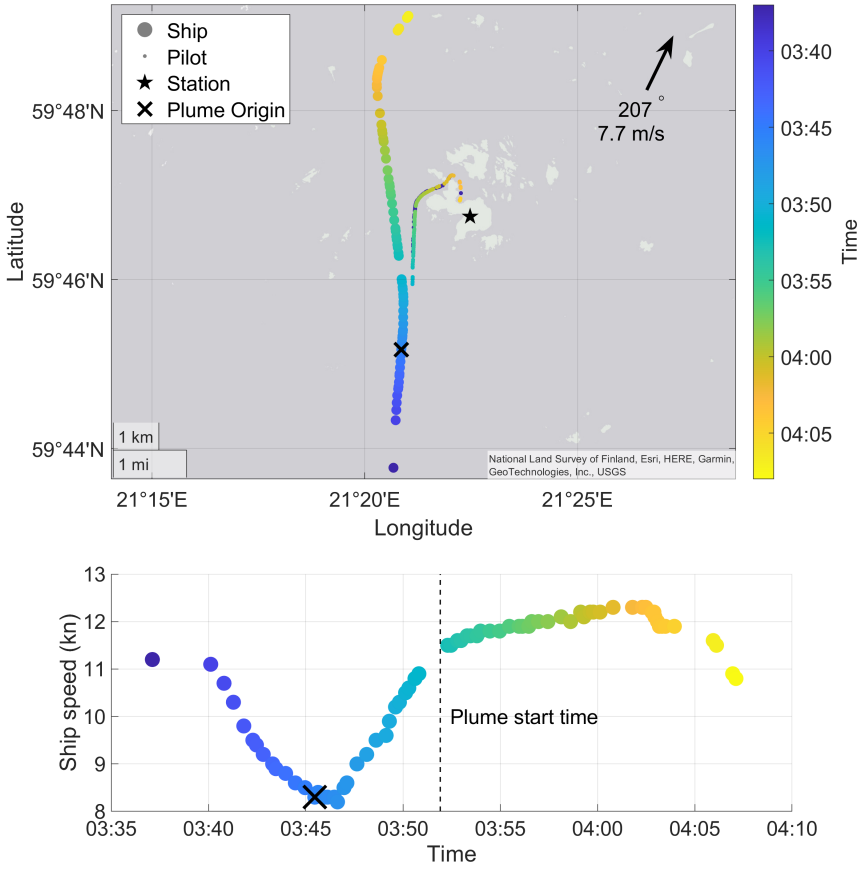

Figure 2. An example of retrieving speed, heading and course over ground information of a passing ship. The upper panel shows the wind direction and speed as well as the location of the ship and the pilot vessel. The location of the air quality station is marked with a star. The lower panel shows the ship speed and time time when the plume was observed at the air quality station. On both panels, the estimated plume origin is marked with a cross and the colouring of the dots on both panels represents the time.

wind was from the direction of the nearest shipping lane ($180° - 360°$). Then the start and end times of the plumes were selected based on the BC and CO_2 data. The typical duration of the plume was a few minutes. Figure 2 shows an example of one ship passing by Utö - data of the ship's location, speed, true heading, and course over the ground were acquired from the AIS data. The plume origin point (a black cross in Fig. 2) was determined based on an assumption that the emission plume was transported to the station directly following the wind direction. Therefore, the closest data point from the direction of the wind was selected to represent the speed, true heading and course over the ground of the ship.

https://doi.org/10.5194/egusphere-2023-2823
Preprint. Discussion started: 12 February 2024

2.3 Black carbon and carbon dioxide measurements

At the Air Quality Station, BC concentration was measured with an aethalometer (Magee Scientific model AE33), and CO_2 concentration with a LI-COR infrared gas analyser (Biosciences model LI-7000). Both of these instruments were installed in the same sample line, which had an inlet on the roof of the measurement cottage roughly at the height of 10 meters from the sea surface (5 meters from the ground level). The sample line had one nafion-dryer installed. The aethalometer and the LI-COR resolutions are 1 min and 5 s, respectively.

BC measurements by an aethalometer are based on filter collection and optical detection. In deriving the BC concentration, a constant mass absorption cross-section, which describes the relation between absorption and BC mass, is assumed. Therefore, based on the recommendations by Petzold et al. (2013), the definition of the measured BC is the so-called equivalent black carbon (eBC). However, for clarity, we use the term BC referring also to the measurements throughout the article. The 880 nm channel with the default mass absorption cross-section of 7.77 $m^2\ g^{-1}$ of the AE33 were used to acquire the BC concentration. Normally, the AE33 data is corrected with a dual-spot correction algorithm, which corrects for measurement artefacts caused by the filter (Drinovec et al., 2015). However, probably due to too high sample relative humidity in the sample line (despite the nafion dryer), the dual-spot correction did not work optimally. Therefore, instead of the dual-spot correction, a correction algorithm suggested by Virkkula et al. (2007) was applied. The correction factors derived by the algorithm were used as 30-day running medians (e.g. Luoma et al., 2021). With this correction scheme, the aethalometer data was more stable and changes in the filter spot did not cause disturbances in the data.

Both BC and CO_2 were converted to dry air and STP conditions (0 °C and 1013.25 hPa) and CO_2 mixing ratio was converted to the same mass unit as BC measurement ($\mu g\ m^{-3}$) using the ideal gas law and the molar mass of CO_2:

$$c_{CO_2}\left(\frac{\mu g}{m^3}\right) = \frac{c_{CO_2}(\mathrm{ppm}) \cdot P \cdot M_{CO_2}}{RT} \quad (1)$$

where c_{CO_2} (g m^{-3}) is the concentration of CO_2 in mass units, c_{CO_2} (ppm) is the mixing ratio of CO_2, P (Pa) is the pressure, M_{CO_2} (44.01 g mol^{-1}) is the molar mass of CO_2, R (8.31 kg m^2 s^{-2} K^{-1} mol^{-1}) is the ideal gas constant and T (K) is the temperature.

Before defining the BC and CO_2 concentrations for each plume, the background levels were subtracted from the BC and CO_2 data. We applied a method introduced by Ausmeel et al. (2019) to calculate the background, which was defined as the median value of 6 minutes before the plume started and 6 minutes after the plume ended omitting the period of the plume. Finally, the dispersed emission ΔBC and ΔCO_2 were calculated as integral over the duration of the plume. Also, a method, which was developed by Kivekäs et al. (2014) and previously applied at Utö to study the effect of sulphur restrictions on aerosol particle number concentration by Seppälä et al. (2021) was tested. In the method, the background is determined as the 25^{th} percentile of 40 consecutive measurements and it suits well automatic plume detection. However, in this application, the method was not optimal due to rather rapid changes in the background levels.

https://doi.org/10.5194/egusphere-2023-2823
Preprint. Discussion started: 12 February 2024

Further, the BC emission factor per fuel consumed EF_{BC} can be defined as a dimensionless ratio of ΔBC and ΔCO_2 times the amount of CO_2 in the exhaust, which is derived from the fuel carbon content (FCC, in kg C/kg fuel):

$$EF_{BC}\left(\frac{\text{kg BC}}{\text{kg fuel}}\right) = \frac{\Delta BC}{\Delta CO_2} \times \frac{M_{CO_2}}{M_C} \times FCC\left(\frac{\text{kg C}}{\text{kg fuel}}\right), \quad (2)$$

where M_{CO_2} is the molar mass of CO_2 (44.01 g mol^{-1}), M_C is the molar mass of carbon (12.01 g mol^{-1}). FCC is 0.85 and 0.87 for HFO and MGO, respectively (IMO Marine Protection Committee, 2018).

2.4 Engine load, fuel consumption and emission factor calculations

211 plumes from 47 different ships representing 10 different vessel types were selected for examination. Ships were identified by Automatic Identification System (AIS) data, and ship-specific details were extracted from the IHS Markit ship database. Vessel actual draughts were extracted from AIS data and compared to design draughts from the IHS Markit ship database. Plumes caused by ships with a ratio between actual draught per design draught < 0.9 were considered to be in ballast condition and others in laden condition. Examined vessels and their specific details are shown in Table 1.

The vessels were categorized based on whether they had an exhaust gas cleaning system (EGCS) installed or not. All vessels had 4-stroke main engines and were expected to use Heavy Fuel Oil (HFO) if equipped with EGCS and very low sulphur Marine Gas Oil (MGO) if not equipped with EGCS. Ships equipped with EGCS could also operate using MGO and with the EGCS switched off, which could explain possible outliers in the data.

Table 1: Vessel type, number of main engines (ME) on board, number of propellers (PR), total main engine power in kW of all main engines fitted on board (kW), built year of the ship (BY), ship service speed as per the IHS Markit database (SS), number of examined exhaust gas plumes (PL), if the ship was fitted with an exhaust gas cleaning system (ES) or not, if the ship has diesel-electric propulsion or not (DE) and if the ship has a shaft generator or not (SG). The vessel marked with * did not have a service speed entry in the ship database and the value was estimated by comparing it to a similar vessel.

N	Vessel	ME	PR	kW	BY	SS	PL	ES	DE	SG
1	Bulk 1	1	1	6252	1995	13.5	1	No	No	Yes
2	Cruise 1	5	2	34560	1993	20.0	3	No	Yes	No
3	Cruise 2	5	2	55216	2000	22.5	1	Yes	Yes	No
4	Cruise 3	4	2	32000	2020	20.0	1	Yes	Yes	No
5	Fish 1	1	1	827	1980	12.0	2	No	No	Yes
6	General cargo 1	1	1	2400	2001	12.0	4	No	No	Yes
7	General cargo 2	1	1	1650	1994	11.0	7	No	No	Yes
8	General cargo 3	1	1	1360	1998	11.0	2	No	No	Yes
9	General cargo 4	1	1	2400	1997	12.0	10	No	No	Yes
10	General cargo 5	1	1	794	2000	10.0	1	No	No	Yes

https://doi.org/10.5194/egusphere-2023-2823
Preprint. Discussion started: 12 February 2024

N	Vessel	ME	PR	kW	BY	SS	PL	ES	DE	SG
11	General cargo 6	1	1	1492	2000	10.7	3	No	No	Yes
12	General cargo 7	1	1	1800	2008	12.0	3	No	No	Yes
13	General cargo 8	1	1	2000	1994	12.5	1	No	No	Yes
14	General cargo 9	1	1	1800	1999	12.5	1	No	No	Yes
15	General cargo 10	1	1	2700	2005	13.0	1	No	No	Yes
16	General cargo 11	1	1	2460	1997	13.5	1	No	No	Yes
17	General cargo 12	1	1	2880	2002	14.0	2	No	No	Yes
18	General cargo 13	1	1	2959	2010	14.0*	1	No	No	No
19	Other 1	2	2	4440	2008	13.0	1	No	Yes	No
20	Other 2	3	2	3600	2012	13.0	1	No	Yes	No
21	Ropax 1	5	2	29880	2001	18.5	3	No	Yes	No
22	Ropax 2	4	2	32580	1991	21.0	1	No	No	No
23	Roro 1	2	2	18900	2002	20.0	9	Yes	No	Yes
24	Roro 2	2	2	25200	2007	22.7	5	Yes	No	Yes
25	Roro 3	2	2	20000	2012	20.0	25	Yes	No	Yes
26	Roro 4	2	2	20000	2012	20.0	24	Yes	No	Yes
27	Roro 5	2	2	20000	2012	20.0	6	Yes	No	Yes
28	Roro 6	2	2	20000	2012	20.0	4	Yes	No	Yes
29	Roro 7	1	1	12600	2000	20.0	6	Yes	No	Yes
30	Roro 8	2	2	25200	2006	22.7	8	Yes	No	Yes
31	Roro 9	2	2	12000	2017	18.0	21	Yes	No	Yes
32	Roro 10	2	2	25200	2008	22.0	7	Yes	No	Yes
33	Roro 11	2	2	25200	2009	22.0	4	Yes	No	Yes
34	Roro 12	2	2	25200	2007	22.7	13	Yes	No	Yes
35	Roro 13	2	2	25200	2006	22.7	5	Yes	No	Yes
36	Tanker 1	1	1	8450	2005	15.3	6	Yes	No	Yes
37	Tanker 2	1	1	4320	2009	14.6	1	No	No	Yes
38	Tanker 3	1	1	5800	2008	14.0	4	No	No	No
39	Tanker 4	1	1	4000	2012	13.0	2	No	No	No
40	Tanker 5	1	1	4000	2012	13.0	1	No	No	No
41	Tanker 6	1	1	5700	2021	14.0	1	No	No	No
42	Tanker 7	1	1	9450	2004	14.5	1	No	No	No
43	Tanker 8	1	1	8450	2004	15.3	1	No	No	Yes
44	Tanker 9	1	1	4320	2006	15.0	3	No	No	No

https://doi.org/10.5194/egusphere-2023-2823
Preprint. Discussion started: 12 February 2024

N	Vessel	ME	PR	kW	BY	SS	PL	ES	DE	SG
45	Tanker 10	1	1	6000	2018	13.0	1	No	No	No
46	Tanker 11	1	1	4000	2011	14.1	1	No	No	No
47	Tug 1	1	1	1839	1976	13.0	1	No	No	No

The apparent wind experienced by the vessel was computed using the true wind speed and direction combined with the heading and speed over ground of the vessel recorded from the AIS data using trigonometry (Kim and Yaakob, 2016). The ambient wind data was used to calculate sea state in Beaufort scale and the added resistance with resulting speed loss created by sea state was calculated by the method created originally by Townsin and Kwon (1983), revised by the same authors (Townsin and Kwon, 1993; Kwon, 2008).

Aerodynamic and hydrodynamic resistance in combined with ship AIS speed data was then used to model the estimated main engine load at the time when the exhaust gas plume data was collected by calculating the resistance through the water using the method created by Hollenbach (1998). Separate resistance constants were used for ships with one or two propellers and ships with and without a bulbous bow. For the calculation of the ship's block coefficient, the method suggested by Jensen (1994) was used to estimate the wet surface of each vessel. Vessel parameters were obtained from the IHS Markit ship database. On ships that have multiple main engines and two propellers, a minimum of two engines were assumed to be online at any time and the maximum engine load before switching on a new engine was set to 90%. For diesel-electric vessels and ships equipped with shaft generators, the estimated auxiliary engine power was added to the main engine power needed for specific speeds. The auxiliary engine power (P_{AE}) was estimated using the International Maritime Organisation Energy Efficiency Design Index (EEDI) formulas (IMO Marine Protection Committee, 2018).

For ships with total installed main engine power $P_{\mathrm{ME}} \geq 10000$ kW:

$$P_{\mathrm{AE}} = 0.025 P_{\mathrm{ME}} + 250 \text{ kW} \tag{3}$$

And for ships with $P_{\mathrm{ME}} \leq 10000$ kW:

$$P_{\mathrm{AE}} = 0.05 P_{\mathrm{ME}} \tag{4}$$

There were 6 diesel-electric ships with multiple engines among the studied vessels (Cruise 1, 2 and 3, Ropax 1, Other 1 and Other 2), many with shaft generators and some with neither. Each ship's main engine power was modelled to its service speed + 5 knots. If the power needed for the speed exceeded the total installed main engine power, the main engine load was set to 100%. A sample of unadjusted modelled engine loads are presented in Fig. 3. It is worth noting that not all vessels use 100% main engine load even at service speed + 5 knots in the model. This is probably true in real life, as for example ships with ice class might have excess engine power as per the ice class demands. Also, vessels designed for towing cargo, such as Tug 1 in the dataset, have more main engine power installed than they would need to reach their design service speed + 5 knots (Figure 3).

The AIS data contains a value for the ship's draught, which is fed to the AIS transmitter from the ship. These values were compared to the design draughts of each vessel. If the ratio of actual draught per design draught was less than 0.9, the vessel

https://doi.org/10.5194/egusphere-2023-2823
Preprint. Discussion started: 12 February 2024

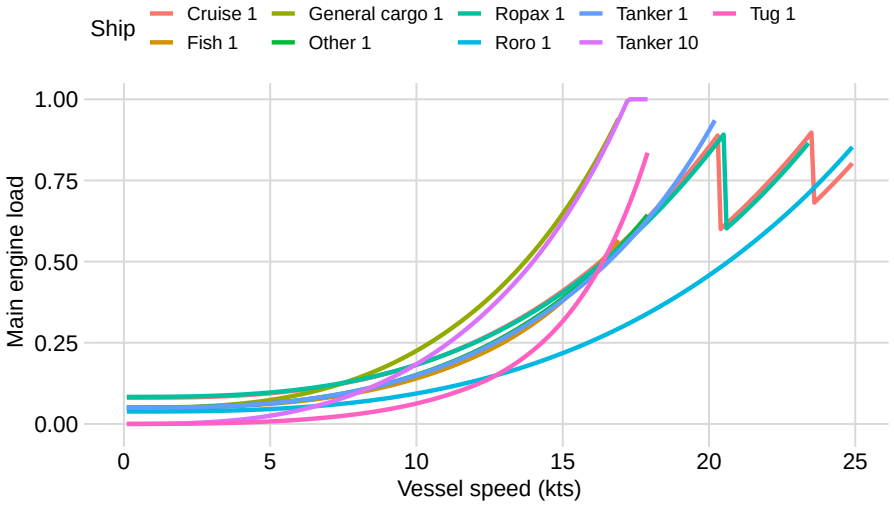

Figure 3. Modelled main engine loads without meteorological parameters of a sample of studied vessels with vessel speed over ground in knots on x-axis and modelled engine load (0-1) on y-axis.

was considered to be in ballast condition and otherwise in laden condition, when passing the measuring site (Figure 4). Two vessels, Tug 1 and Fish 1, reported actual draughts that were significantly larger than their design draughts, which could be caused by user error or error in the ship database. Smaller exceeding of the design draught could be because of trim or water density, which is usually around 1.010 t m^{-3} in the Baltic Sea and the design draught is calculated for a water density of 1.025 t m^{-3}. Actual draughts and water density of 1.010 t m^{-3} were used in the modelling of resistance through the water.

Modelled main engine load and measured BC values from ship plumes were analysed for correlation and to create statistical models to estimate emissions created by changes in speed and main engine load. The obtained regression formula coefficients for BC output ($g\,BC\,(kg\,fuel)^{-1}$) as a function of engine load were used to model the absolute BC emission ($g\,BC\,h^{-1}$) as a function of speed. For this, the main engine fuel consumption (F_{ME}) of each ship was modelled using a base-specific fuel oil consumption ($SFOC_{Base}$) in g kWh^{-1} obtained from the IHS Markit ship database for the specific ship multiplied by the unitless generic relative specific fuel oil consumption ($SFOC_{Relative}$) described by Jalkanen et al. (2012):

$$F_{ME} = SFOC_{Base} \times SFOC_{Relative}, \tag{5}$$

where

$$SFOC_{Relative} = (\alpha L^2 + \beta L + \gamma) \tag{6}$$

where L is the engine load (0-1), α = 0. 45, β = -0.71, and γ = 1.28. BC emission (g h^{-1}) was then calculated as:

$$BC_s\left(\frac{g}{h}\right) = F_{ME}\left(\frac{g\ fuel}{kWh}\right) * P_{ME}(kW) * BC_L\left(\frac{g\ BC}{g\ fuel}\right) \tag{7}$$

https://doi.org/10.5194/egusphere-2023-2823
Preprint. Discussion started: 12 February 2024

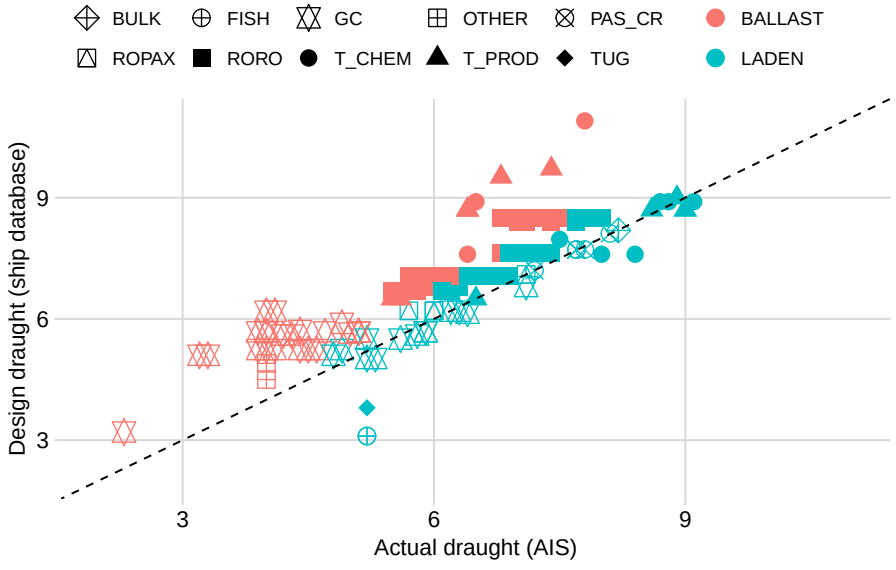

Figure 4. Actual draughts of studied vessels (x-axis) compared to design draughts (y-axis) from the IHS Markit ship database in metres. Different vessel types are indicated with corresponding shapes. Vessels in laden condition in green and in ballast condition in orange.

where BC_s is the BC output (g h^{-1}) for a specific speed, F_{ME} is the main engine fuel consumption for a specific speed (g fuel kWh^{-1}), P_{ME} is the modelled main engine power need for specific speed and BC_L is the load-specific BC output ($g\,BC\,(kg\,fuel)^{-1}$).

BC output in g per nautical mile (NM) was calculated as:

$$BC_d\left(\frac{g}{NM}\right) = \frac{BC_s(\frac{g}{h})}{S(\frac{NM}{h})} \quad (8)$$

where BC_d is the BC output in grams per NM, BC_s is the BC output in grams per hour and S is the speed of the vessel in NM per hour.

Vessel total greenhouse gas emissions were calculated using 20 and 100-year global warming potential (GWP_{20} and GWP_{100}) of BC, estimated as 2200 and 680 (Bond and Sun, 2005) in combination with vessel CO_2 emissions to determine the effect of speed change in the total GHG as CO_2 equivalent (CO_2e). Emission factors used for CO_2 were 3.11 for HFO and 3.21 for MGO (MEPC, 2021). The code for modelling the engine load was created using Python programming language. The data analysis was performed in R (version 4.2.1) and plotted using the Ggplot2 package (Wickham, 2009).

https://doi.org/10.5194/egusphere-2023-2823
Preprint. Discussion started: 12 February 2024

3 Results

3.1 Black carbon emission factors

Vessels equipped with Exhaust Gas Cleaning System (EGCS) emit significantly less BC (mean: 0.22 $\mathrm{g\,BC\,(kg\,fuel)^{-1}}$, standard deviation: 0.21) than vessels without EGCS (mean: 0.99 $\mathrm{g\,BC\,(kg\,fuel)^{-1}}$, SD: 0.68). Statistical significance was confirmed with the Welch Two Sample t-test ($p < 0.01$). There is no statistically significant difference ($p = 0.63$) between BC emissions of ships in ballast condition (mean: 0.50 $\mathrm{g\,BC\,(kg\,fuel)^{-1}}$, SD: 0.50) and ships in laden condition (mean: 0.44 $\mathrm{g\,BC\,(kg\,fuel)^{-1}}$, SD: 0.63). Ships with service speeds > 15.0 knots emit significantly ($p < 0.01$) less BC (mean: 0.25 $\mathrm{g\,BC\,(kg\,fuel)^{-1}}$, SD: 0.24) than ships with service speeds < 15.0 knots (mean: 1.06 $\mathrm{g\,BC\,(kg\,fuel)^{-1}}$, SD: 0.71). Vessel type BC emission factors are presented in Table 2 and in Fig. 5.

Table 2. Vessel type, mean BC emission factor ($\mathrm{EF_{BC}}$) in the unit $\mathrm{g\,BC\,(kg\,fuel)^{-1}}$, standard deviation (SD), and number of examined vessels (N). There was only one bulk carrier and one tug with one plume each in the dataset and therefore standard deviation could not be calculated.

Vessel type	$\mathrm{EF_{BC}}\left(\frac{\mathrm{g\ BC}}{\mathrm{kg\ fuel}}\right)$	$\mathrm{SD}\left(\frac{\mathrm{g\ BC}}{\mathrm{kg\ fuel}}\right)$	N
Bulk	0.20	na	1
Chemical tanker	0.72	0.40	10
Cruise	0.31	0.21	5
Fish	1.18	0.50	2
General cargo	1.19	0.63	37
Other	0.38	0.04	2
Product tanker	0.75	0.18	12
Ropax	0.37	0.47	4
Roro	0.22	0.20	137
Tug	3.91	na	1
All vessels	0.48	0.56	211

3.2 Correlation analysis

Vessel speed over ground has a strong negative Pearson's correlation between BC emission factor of -0.67 (95% confidence interval -0.73–-0.58, $p > 0.01$). The correlation between speed and BC emission factor on ships with EGCS was -0.60 (95% confidence interval -0.70–-0.49, $p > 0.01$) and on ships without EGCS it was -0.32 (95% confidence interval -0.51–-0.09, $p = 0.01$). The correlation between speed over ground and BC emission factor on ships with service speeds > 15.0 knots was -0.69 (95% confidence interval -0.76–-0.59, $p < 0.01$) and on ships with service speeds < 15.0 knots -0.21 (95% confidence interval -0.44–0.05, $p = 0.12$). The correlation between speed over ground and BC emission factor on ships

https://doi.org/10.5194/egusphere-2023-2823
Preprint. Discussion started: 12 February 2024

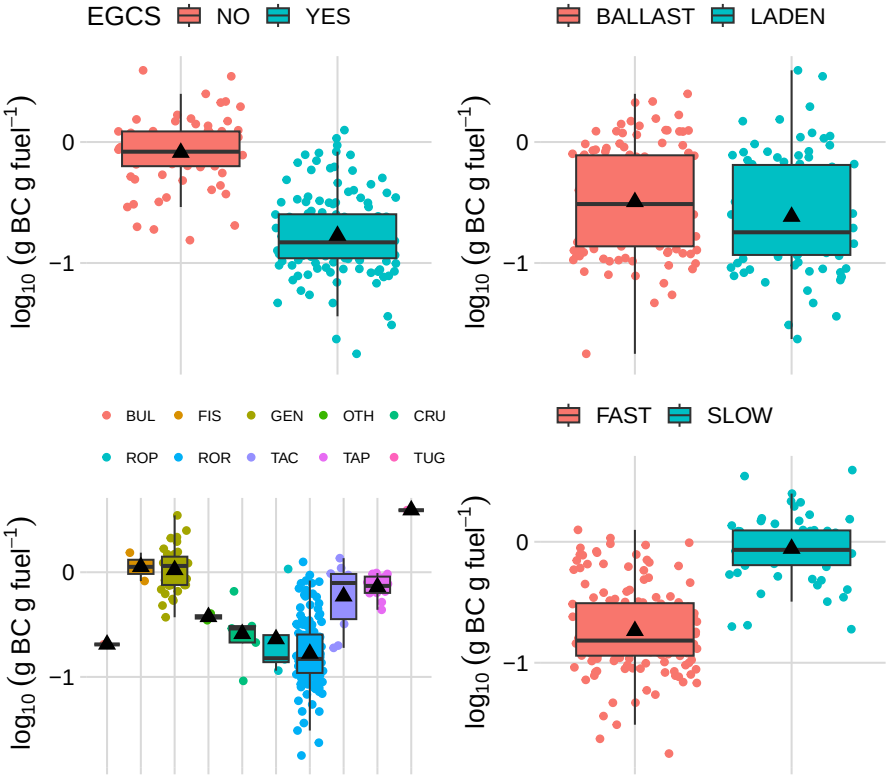

Figure 5. Boxplots of the emission factor $\log_{10}$ (g BC (kg fuel)$^{-1}$) measured from passing ships grouped by having an Exhaust Gas Cleaning Systems (top left), by being in ballast or laden condition (top right), having a service speed larger or less than 15.0 knots (bottom right) or by vessel type (bottom left) showing median as black line with interquartile ranges, outliers and means with black triangles. BUL: bulk carrier, FIS: fishing vessel, GEN: general cargo vessel, OTH: other vessel type, CRU: cruise passenger vessel, ROP: ropax vessel, ROR: roro vessel, TAC: chemical tanker, TAP: product tanker, TUG: tug.

in ballast condition was -0.72 (95% confidence interval -0.80–-0.62, $p < 0.01$) and on ships in laden condition it was -0.63 (95% confidence interval -0.74–-0.49, $p < 0.01$).

Tug1 which had only one exhaust gas plume in the dataset and passed the measuring site at a very low speed has an emission factor 4 times larger than the mean for vessels without EGCS. A visual confirmation from the automatic camera at the measuring site confirmed that Tug1 was towing a barge while passing Utö. As modelling the engine load was impossible, Tug1 was removed from further analysis, leaving 210 plumes in the dataset. All except for one vessel passing the measuring site with a speed > 15 knots over the ground were equipped with EGCS. Most vessels without EGCS were also ships with lower service speeds and therefore would not need to slow down for the pilot exchange. They also emit more BC than the EGCS-equipped vessels and therefore create bias in the analysis if included. Further analyses were performed only for the EGCS-equipped vessels using 142 exhaust gas plumes and three different vessel types in the dataset.

https://doi.org/10.5194/egusphere-2023-2823
Preprint. Discussion started: 12 February 2024

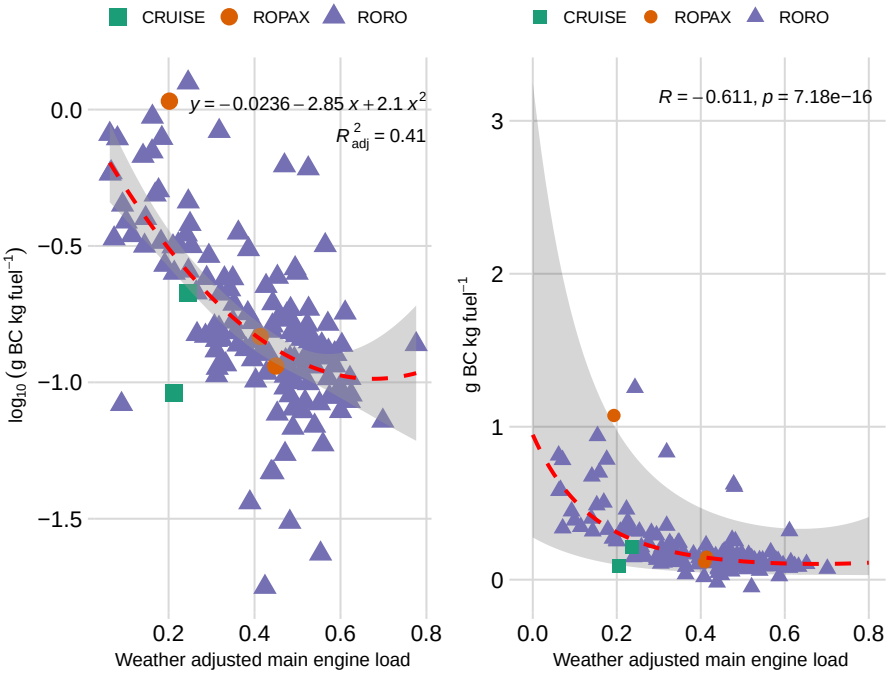

Figure 6. Left: scatterplot of $\log_{10}$ BC emission factor (g kg fuel^{-}1) as a function of weather adjusted main engine load with 2^{nd} degree polynomial regression (red dashed line) and 95% confidence interval (grey area). Right: BC emission factor (g kg fuel^{-}1) with the same regression (red dashed line) and 95% prediction interval (grey area).

3.3 Emission factor as a function of engine load

Visual examination combined with knowledge from previous literature confirmed a non-linear relationship between modelled engine load and BC emission factor. To define the emission factor of BC as a function of engine load, 2^{nd} degree polynomial regression was fitted to the logarithm of observed and modelled values. Adjusting for meteorological parameters had a small effect when fitting the regression. In the exhaust gas plumes emitted by EGCS-equipped vessel, the correlation between unadjusted modelled engine load and BC emission factor was -0.61 (95% confidence interval -0.70–-0.50, $p < 0.01$) and the goodness of fit (adjusted r^2) of the polynomial regression was 0.46. When the engine load was adjusted for weather conditions, the correlation between engine load and BC emission factor was -0.61 (95% confidence interval -0.69 - -0.48, $p > 0.01$) and the adjusted r^2 of the polynomial regression was 0.41. The obtained load-based emission factor formula for the BC output from EGCS-equipped vessels is:

$$\log_{10}(\mathrm{LEF_{BC}}) = 2.10L^2 - 2.85L - 0.02 \quad (9)$$

where $\mathrm{LEF_{BC}}$ is the load-based BC emission factor (g kg fuel^{-}1) and L is the engine load (0-1) (Fig. 6).

https://doi.org/10.5194/egusphere-2023-2823
Preprint. Discussion started: 12 February 2024

3.4 Total greenhouse gas emissions at various speeds

As shown above, the fuel consumption-based BC emissions from ships that are equipped with EGCS are dependent on the engine load. As the engine load varies with different power demands, which again is dependent on the speed of the vessel, BC emissions can be modelled as a function of vessel speed. Five different ships representing various vessel types were chosen as a sample from the studied vessels. Three of them have conventional propulsion systems (Roro1, Roro2 and Tanker), which means the main engines are connected mechanically to the propeller shaft. The other two (Ropax and Cruise) are diesel-electric, which means the main engines are connected to generators, and propellers are rotated with electric motors. 80% engine load was chosen as cut-off, as the data from our observations was limited to around 80% modelled engine load. Chosen vessels also had different specific fuel oil consumption ($SFOC_{Base}$) based on the ship database information varying from 180 to 220 g kWh^{-1}.

BC emission was modelled as grams per hour and as grams per nautical mile to distinguish between service speed and reduced speed. Due to the parabolic models for fuel consumption and BC emission factor curves, BC emissions increase non-linearly from when the ship starts moving until reaching the first peak, which seems to be at around 10-12 knots speed. BC emissions then decrease until reaching similar levels than at 5-knot speed. This seems to happen at around the ship service speed, from where the BC emissions seem to increase again. Vessel service speed is reached where main engine fuel consumption is around $SFOC_{Base}$ this being typically around 60-80% load for most marine engines. Within the modelled vessels, this would be at around 15-20 knots speed. Increasing speed further also increases the BC emissions non-linearly. Total greenhouse gas emissions are dominated by CO_2 and are reduced non-linearly with a reduction of speed (Fig. 7).

https://doi.org/10.5194/egusphere-2023-2823
Preprint. Discussion started: 12 February 2024

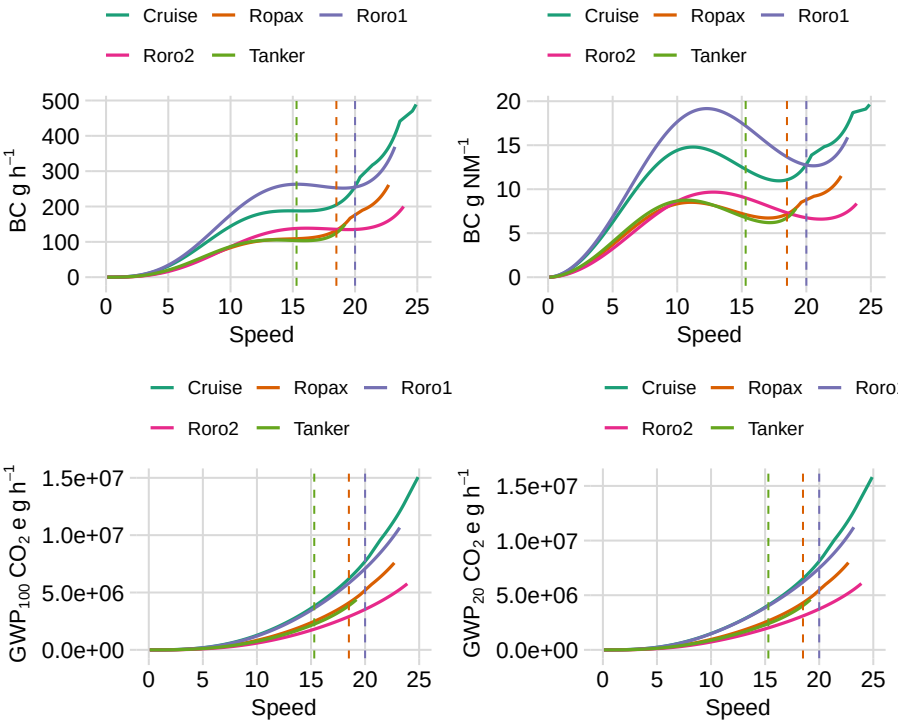

Figure 7. BC emission (g h^{-1}) as a function of speed of 5 different modelled ships (top left), BC emissions (g per nautical mile) of the same vessels as a function of speed (top right), total greenhouse gas emissions (CO_2 + BC) using global warming potential for 100 years for BC (bottom left) and with global warming potential for 20 years (bottom right). Vessel service speeds as vertical dashed lines. Vessels Cruise, Roro1 and Roro2 has the same service speed (20.0 knots).

4 Discussion

The mean BC emission factor derived from the aethalometer measurements for all examined ship exhaust gas plumes (0.48 ± 0.56 g BC $(\mathrm{kg\,fuel})^{-1}$) and vessel type-specific means (Table 2) are in line with the results from previous literature using various measuring methods: Schlaerth et al. (2021) measured 78 plumes using a custom-built light absorption photometer obtaining a mean emission factor of 0.49 ± 0.62 g BC $(\mathrm{kg\,fuel})^{-1}$ from onshore measurements of various harbour crafts, Cappa et al. (2014) used a single particle photometer and a soot-particle aerosol mass spectrometer to calculate a weighted average of 0.23 ± 0.15 g BC $(\mathrm{kg\,fuel})^{-1}$ for the research vessel *Miller Freeman*. Buffaloe et al. (2013) measured 91 ship plumes from onboard a research vessel combining multiple techniques (photoacoustic spectrometer and particle soot absorption photometer for light absorption, laser-induced incandescence and mass spectrometry) obtaining a weighted mean for all ships of 0.31 ± 0.31 g BC $(\mathrm{kg\,fuel})^{-1}$, 0.26 ± 0.26 for ships with slow-speed diesel engines (SSD), 0.27 ± 0.12 for ships with medium-speed diesel engines (MSD) and 0.32 ± 0.26 for ships with high-speed diesel engines (HSD). Lack et al. (2008) measured 101 ship plumes from onboard a research vessel using a photoacoustic technique to calculate the light absorbing carbon obtaining emission

https://doi.org/10.5194/egusphere-2023-2823
Preprint. Discussion started: 12 February 2024

factors 0.41 ± 0.27 g BC (kg fuel)$^{-1}$ for SSD-powered ships, 0.97 ± 0.66 for MSD-powered ships and 0.36 ± 0.23 for HSD-powered ships with vessel-specific emission factors: 0.38 ± 0.27 for tankers, 0.80 ± 0.23 for containerships, 0.40 ± 0.23 for cargo carriers, 0.38 ± 0.16 for bulk carriers, 0.97 ± 0.66 for tug boats and 0.36 ± 0.23 for passenger boats. Petzold et al. (2008) used a particle soot absorption photometer and measured 0.17 ± 0.04 g BC (kg fuel)$^{-1}$ from a single containership with aeroplane measurements, Sinha et al. (2003) used an aeroplane to collect filter samples from plumes of a tanker and a containership. The filters were analysed with an optical transmission technique obtaining a mean emission factor of 0.18 ± 0.02 g BC (kg fuel)$^{-1}$.

As seen above, BC concentration can be measured by various methods that rely on the different properties of the BC (e.g, chemical composition, refractivity or optical properties), they are based on different assumptions (e.g., mass absorption cross-section, calibrations), and they are sensitive to different measurement artefacts (errors caused by e.g., relative humidity, filter fibres, other absorbing substances) (Petzold et al., 2013). A study by Aakko-Saksa et al. (2022) investigated various methods to measure BC emissions in a laboratory and on-board. In their results, BC concentration measured by an aethalometer showed about 1.26 times more than the other used methods (filter smoke number, laser-induced incandescence, photoacoustic spectroscopy). On an on-board BC measurement comparison by Cappa et al. (2014) the laser-induced incandescence showed somewhat lower results to other methods (optical, photoacoustic). Also, Buffaloe et al. (2013) observed that laser-induced incandescence measurements resulted in lower BC emission factors than those measured by optical means on a plume-chasing measurement campaign. Not only did the method to measure BC vary, but also the measurement set-up varied; some studies measured the in-stack emissions of a certain ship and others measured the emissions of various ships by either chasing the plumes or measuring the plumes from passing ships. When measuring emission plumes, the emissions are not as fresh when measured in-stack. Even though BC is an inert compound and its chemical composition is not expected to change, it can still get coated with other materials during ageing that affect the optical properties of BC particles. For example, purely scattering or slightly absorbing coating can increase the light absorption of the coated BC particle (Bond et al., 2006; Lack and Cappa, 2010). This so-called lensing effect can lead to an overestimation of BC concentration, when BC is derived by optical methods and a constant mass absorption cross section (for fresh emissions) is used.

Here, we assumed that the BC particle ageing has only a minor effect on the optically derived BC concentration. The lag time between the plume emission from the stack and detection by the analyzer was less than 5 minutes on average. Only a few of the plumes travelled more than 10 minutes before detection. There was no correlation between the $\mathrm{EF_{BC}}$ and the plume age during this short time period in the marine background station. Even on longer time scales, previous studies have observed the low potential for new particulate material formation in photo-oxidation processes in the exhaust of EGCS-equipped ships (Karjalainen et al., 2022) and for ship emissions in SECA area (Ausmeel et al., 2020). Previously, at Utö, Seppälä et al. (2021) suggested diminished photochemical ageing of the plumes with stricter fuel sulphur restrictions.

In the studies mentioned above that observed BC emissions from ships, the ship fleet varied a lot and most of the studies included ships with different service speeds and that operated with low sulphuric fuels. Here, the focus was on ships with service speeds over 15 knots and that were equipped with an EGCS. As the use of EGCSs has been increasing, it underlines the importance of studying also their emissions.

https://doi.org/10.5194/egusphere-2023-2823
Preprint. Discussion started: 12 February 2024

Ships without EGCS had a mean BC emission factor of almost 5-fold larger than vessels with EGCS, which is also in line with previous known literature (Lack and Corbett, 2012; Lehtoranta et al., 2019). The dataset used was dominated by EGCS-equipped vessels, for which reason all further analyses were focused only on EGCS vessels to avoid bias in the results. Therefore, no conclusions can be made concerning ships without EGCS from this study. Further research is needed to determine the load-based emission factor formula for slow-moving vessels without EGCS.

Meteorological parameters have a significant effect on the resistance experienced by the vessel while navigating and they should be taken into account when modelling engine load based on AIS data. As there is no tidal flow at the research site, the effect of currents was omitted in the modelling. The speed penalty calculation developed by Kwon (2008) which was used in this study classifies ships by their Froude number and whether they are in ballast or laden condition. A distinction is also made between container ships and other vessel types. A similar method developed by Jalkanen et al. (2009) was also tried, but it rendered results that were less accurate than Kwon's method. Using actual reported draughts instead of the design draught from a ship database adds to the accuracy of the modelling as it can be used to differentiate ships in ballast and laden conditions.

Most of the vessels in this study were either diesel-electric or were equipped with shaft generators. Therefore, the estimated auxiliary power was added to the modelled main engine power and contributed to the modelled main engine load. However, as it was impossible to distinguish if the shaft generators were in use or not, the measured plumes were a mix of the main engine and possible auxiliary engine exhaust gases. We estimate, that this should not cause significant bias in the results as the vessels with the largest auxiliary demand (cruise and ropax vessels) were mostly also diesel-electric and not equipped with separate auxiliary engines.

5 Conclusions

The mean black carbon emission factor (EF_{BC}) for 47 ships representing 10 different vessel types measured from a remote marine station was 0.48 ± 0.56 g BC $(\mathrm{kg\,fuel})^{-1}$. For ships equipped with EGCS it was 0.22 ± 0.21 and for ships without EGCS 0.99 ± 0.68. EF_{BC} has a strong negative correlation with speed and engine load, which can be modelled to a reasonable degree of accuracy. Based on the results of this study, reducing vessel speed will result in a reduction of greenhouse gas emissions at least for EGCS-equipped vessels powered by fuel oil. However, local speed restrictions might not be beneficial: if speed is increased during the remaining voyage the overall GHG emissions might be more than without the speed restriction. Also, as BC emissions have other effects, such as on human health, local BC concentrations are increased with small reductions in speed. Based on the results, speed limits need to be 10 knots or less for the BC emissions to be the same as with the ship's normal service speeds. This should be considered carefully at locations where the human population are exposed to ship exhaust gas plumes.

https://doi.org/10.5194/egusphere-2023-2823
Preprint. Discussion started: 12 February 2024

Author contributions. Conceptualization: M.H., T.M. Data curating: T.M., K.L. Formal Analysis: M.H., T.M., K.L. Investigation: T.M, K.L. Methodology: M.H. Project administration: M.H., T.G. Resources: T.M. Software: M.H., K.L. Supervision: T.G. Validation: M.H., T.G. Visualization: M.H. Writing original draft: M.H., T.G. Writing – review and editing: All authors.

Competing interests. The authors declare that they have no conflict of interest

Disclaimer. This work reflects only the authors' view and CINEA is not responsible for any use that may be made of the information it contains.

Acknowledgements. This research was produced as part of the European Union project "EMERGE: Evaluation, control, and mitigation of the environmental impacts of shipping emissions". The EMERGE project has received funding from the European Union's Horizon 2020 – Research and Innovation Framework Programme action under grant agreement No 874990. Observations and research support at Utö Atmosphere and Marine Research Station are partly funded by Integrated Carbon Observing System (ICOS) and the Finnish Marine Research Infrastructure (FINMARI). Special thanks are due to Ismo and Brita Willström for their valuable work in maintenance of the measurements at Utö.

https://doi.org/10.5194/egusphere-2023-2823
Preprint. Discussion started: 12 February 2024

References

Aakko-Saksa, P., Kuittinen, N., Murtonen, T., Koponen, P., Aurela, M., Järvinen, A., Teinilä, K., Saarikoski, S., Barreira, L. M. F., Salo, L., Karjalainen, P., Ortega, I. K., Delhaye, D., Lehtoranta, K., Vesala, H., Jalava, P., Rönkkö, T., and Timonen, H.: Suitability of Different Methods for Measuring Black Carbon Emissions from Marine Engines, Atmosphere, 13, https://doi.org/10.3390/atmos13010031, 2022.

Almström, B. and Larson, M.: Measurements and analysis of primary ship waves in the Stockholm Archipelago, Sweden, Journal of Marine Science and Engineering, 8, 1–23, https://doi.org/10.3390/JMSE8100743, 2020.

Almström, B., Roelvink, D., and Larson, M.: Predicting ship waves in sheltered waterways – An application of XBeach to the Stockholm Archipelago, Sweden, Coastal Engineering, 170, https://doi.org/10.1016/J.COASTALENG.2021.104026, 2021.

Almström, B., Larson, M., and Hallin, C.: Decision support tool to mitigate ship-induced erosion in non-uniform, sheltered coastal fairways, Ocean & Coastal Management, 225, 106 210, https://doi.org/10.1016/J.OCECOAMAN.2022.106210, 2022.

Ausmeel, S., Eriksson, A., Ahlberg, E., and Kristensson, A.: Methods for identifying aged ship plumes and estimating contribution to aerosol exposure downwind of shipping lanes, Atmospheric Measurement Techniques, 12, 4479–4493, https://doi.org/10.5194/amt-12-4479-2019, 2019.

Ausmeel, S., Eriksson, A., Ahlberg, E., Sporre, M. K., Spanne, M., and Kristensson, A.: Ship plumes in the Baltic Sea Sulfur Emission Control Area: chemical characterization and contribution to coastal aerosol concentrations, Atmospheric Chemistry and Physics, 20, 9135–9151, https://doi.org/10.5194/acp-20-9135-2020, 2020.

Benassai, G., Piscopo, V., and Scamardella, A.: Field study on waves produced by HSC for coastal management, Ocean & Coastal Management, 82, 138–145, https://doi.org/10.1016/J.OCECOAMAN.2013.06.003, 2013.

Bilkovic, D. M., Mitchell, M. M., Davis, J., Herman, J., Andrews, E., King, A., Mason, P., Tahvildari, N., Davis, J., and Dixon, R. L.: Defining boat wake impacts on shoreline stability toward management and policy solutions, Ocean and Coastal Management, 182, https://doi.org/10.1016/j.ocecoaman.2019.104945, 2019.

Bond, T. C. and Sun, H.: Can Reducing Black Carbon Emissions Counteract Global Warming?, Environmental Science & Technology, 39, 5921–5926, https://doi.org/10.1021/es0480421, 2005.

Bond, T. C., Habib, G., and Bergstrom, R. W.: Limitations in the enhancement of visible light absorption due to mixing state, Journal of Geophysical Research, 111, D20 211, https://doi.org/10.1029/2006JD007315, 2006.

Buffaloe, G., Lack, D. A., Williams, E. J., Coffman, D. J., Hayden, K., Lerner, B. M., Li, S.-M., Nuaaman, I., Massoli, P., Onasch, T. B., Quinn, P. K., and Cappa, C. D.: Black carbon emissions from in-use ships: a California regional assessment, Atmospheric Chemistry and Physics, 14, 1881–1896, https://api.semanticscholar.org/CorpusID:46792307, 2013.

Cappa, C. D., Williams, E. J., Lack, D. A., Buffaloe, G. M., Coffman, D., Hayden, K. L., Herndon, S. C., Lerner, B. M., Li, S.-M., Massoli, P., McLaren, R., Nuaaman, I., Onasch, T. B., and Quinn, P. K.: A case study into the measurement of ship emissions from plume intercepts of the NOAA ship Miller Freeman, Atmospheric Chemistry and Physics, 14, 1337–1352, https://doi.org/10.5194/acp-14-1337-2014, 2014.

Chen, J. and Hoek, G.: Long-term exposure to PM and all-cause and cause-specific mortality: A systematic review and meta-analysis, Environment International, 143, 105 974, https://doi.org/10.1016/J.ENVINT.2020.105974, 2020.

Corbin, J. C., Peng, W., Yang, J., Sommer, D. E., Trivanovic, U., Kirchen, P., Miller, J. W., Rogak, S., Cocker, D. R., Smallwood, G. J., Lobo, P., and Gagné, S.: Characterization of particulate matter emitted by a marine engine operated with liquefied natural gas and diesel fuels, Atmospheric Environment, 220, 117 030, https://doi.org/10.1016/J.ATMOSENV.2019.117030, 2020.

https://doi.org/10.5194/egusphere-2023-2823
Preprint. Discussion started: 12 February 2024

Dam, K. T., Tanimoto, K., and Fatimah, E.: Investigation of ship waves in a narrow channel, Journal of Marine Science and Technology, 13, 223–230, https://doi.org/10.1007/s00773-008-0005-6, 2008.

Drinovec, L., Močnik, G., Zotter, P., Prévôt, A. S. H., Ruckstuhl, C., Coz, E., Rupakheti, M., Sciare, J., Müller, T., Wiedensohler, A., and Hansen, A. D. A.: The "dual-spot" Aethalometer: an improved measurement of aerosol black carbon with real-time loading compensation, Atmospheric Measurement Techniques, 8, 1965–1979, https://doi.org/10.5194/amt-8-1965-2015, 2015.

Elkafas, A. G. and Shouman, M. R.: Assessment of Energy Efficiency and Ship Emissions from Speed Reduction Measures on a Medium Sized Container Ship, International Journal of Maritime Engineering, 163, https://doi.org/10.5750/ijme.v163iA3.805, 2021.

Gunnel, G., Magnus, L., and Jonas, A.: Ship-Generated Waves and Induced Turbidity in the Göta Älv River in Sweden, Journal of Waterway, Port, Coastal, and Ocean Engineering, 140, 04014 004, https://doi.org/10.1061/(ASCE)WW.1943-5460.0000224, doi: 10.1061/(ASCE)WW.1943-5460.0000224, 2014.

Hollenbach, K. U.: Estimating Resistance and Propulsion for Single-Screw and Twin-Screw Ships, vol. 45.2, Ship technology research, 7 edn., 1998.

Houser, C.: Relative importance of vessel-generated and wind vaves to salt marsh Erosion in a restricted fetch environment, Journal of Coastal Research, 26, 230–240, https://doi.org/10.2112/08-1084.1, 2010.

IMO Marine Protection Committee: 2018 Guidelines on the method of calculation of the attained energy efficiency design index (EEDI) for new ships, MEPC/73/19, 1, 11–11, 2018.

Jalkanen, J. P., Brink, A., Kalli, J., Pettersson, H., Kukkonen, J., and Stipa, T.: A modelling system for the exhaust emissions of marine traffic and its application in the Baltic Sea area, Atmospheric Chemistry and Physics, 9, 9209–9223, https://doi.org/10.5194/acp-9-9209-2009, 2009.

Jalkanen, J.-P., Johansson, L., Kukkonen, J., Brink, A., Kalli, J., and Stipa, T.: Extension of an assessment model of ship traffic exhaust emissions for particulate matter and carbon monoxide, Atmospheric Chemistry and Physics, 12, 2641–2659, https://doi.org/10.5194/acp-12-2641-2012, 2012.

Jalkanen, J.-P., Johansson, L., Andersson, M. H., Majamäki, E., and Sigray, P.: Underwater noise emissions from ships during 2014–2020, Environmental Pollution, 311, 119 766, https://doi.org/https://doi.org/10.1016/j.envpol.2022.119766, 2022.

Jensen, G.: Moderne Schiffslinien, vol. 22, Hansa-Verlag, handbuch der werften edn., 1994.

Jiang, Y., Yang, J., Gagné, S., Chan, T. W., Thomson, K., Fofie, E., Cary, R. A., Rutherford, D., Comer, B., Swanson, J., Lin, Y., Rooy, P. V., Asa-Awuku, A., Jung, H., Barsanti, K., Karavalakis, G., Cocker, D., Durbin, T. D., Miller, J. W., and Johnson, K. C.: Sources of variance in BC mass measurements from a small marine engine: Influence of the instruments, fuels and loads, Atmospheric Environment, 182, 128–137, https://doi.org/10.1016/J.ATMOSENV.2018.03.008, 2018.

Karjalainen, P., Teinilä, K., Kuittinen, N., Aakko-Saksa, P., Bloss, M., Vesala, H., Pettinen, R., Saarikoski, S., Jalkanen, J. P., and Timonen, H.: Real-world particle emissions and secondary aerosol formation from a diesel oxidation catalyst and scrubber equipped ship operating with two fuels in a SECA area, Environmental Pollution, 292, https://doi.org/10.1016/j.envpol.2021.118278, 2022.

Kim, T. and Yaakob, O.: Adaptation of wind power for ship essential service system onboard, Journal of Transport System Engineering, 1, 2016.

Kim, Y.-R., Steen, S., Kramel, D., Muri, H., and Strømman, A. H.: Modelling of ship resistance and power consumption for the global fleet: The MariTEAM model, Ocean Engineering, 281, 114 758, https://doi.org/10.1016/J.OCEANENG.2023.114758, 2023.

https://doi.org/10.5194/egusphere-2023-2823
Preprint. Discussion started: 12 February 2024

Kivekäs, N., Massling, A., Grythe, H., Lange, R., Rusnak, V., Carreno, S., Skov, H., Swietlicki, E., Nguyen, Q. T., Glasius, M., and Kristensson, A.: Contribution of ship traffic to aerosol particle concentrations downwind of a major shipping lane, Atmospheric Chemistry and Physics, 14, 8255–8267, https://doi.org/10.5194/acp-14-8255-2014, 2014.

Kwon, Y.: Speed loss due to added resistance in wind and waves, Naval Architect, pp. 14–16, 2008.

Laakso, L., Mikkonen, S., Drebs, A., Karjalainen, A., Pirinen, P., and Alenius, P.: 100 years of atmospheric and marine observations at the Finnish Utö Island in the Baltic Sea, Ocean Science, 14, 617–632, https://doi.org/10.5194/os-14-617-2018, 2018.

Lack, D., Lerner, B., Granier, C., Baynard, T., Lovejoy, E., Massoli, P., Ravishankara, A. R., and Williams, E.: Light absorbing carbon emissions from commercial shipping, Geophysical Research Letters, 35, https://doi.org/10.1029/2008GL033906, 2008.

Lack, D. A. and Cappa, C. D.: Impact of brown and clear carbon on light absorption enhancement, single scatter albedo and absorption wavelength dependence of black carbon, Atmospheric Chemistry and Physics, 10, 4207–4220, https://doi.org/10.5194/acp-10-4207-2010, 2010.

Lack, D. A. and Corbett, J. J.: Black carbon from ships: a review of the effects of ship speed, fuel quality and exhaust gas scrubbing, Atmospheric Chemistry and Physics, 12, 3985–4000, https://doi.org/10.5194/acp-12-3985-2012, 2012.

Lajaunie, M., Ollivier, B., Ceyrac, L., Dellong, D., and Courtois, F. L.: Large-Scale Simulation of a Shipping Speed Limitation Measure in the Western Mediterranean Sea: Effects on Underwater Noise, Journal of Marine Science and Engineering, 11, 251, https://doi.org/10.3390/jmse11020251, 2023.

Lehtoranta, K., Aakko-Saksa, P. I., Murtonen, T., Vesala, H., Ntziachristos, L., Ro¨, T., Karjalainen, P., Kuittinen, N., and Timonen, H.: Particulate Mass and Nonvolatile Particle Number Emissions from Marine Engines Using Low-Sulfur Fuels, Natural Gas, or Scrubbers, Environ. Sci. Technol, 53, 27, https://doi.org/10.1021/acs.est.8b05555, 2019.

Lepistö, T., Kuuluvainen, H., Lintusaari, H., Kuittinen, N., Salo, L., Helin, A., Niemi, J. V., Manninen, H. E., Timonen, H., Jalava, P., Saarikoski, S., and Rönkkö, T.: Connection between lung deposited surface area (LDSA) and black carbon (BC) concentrations in road traffic and harbour environments, Atmospheric Environment, 272, 118 931, https://doi.org/10.1016/J.ATMOSENV.2021.118931, 2022.

Linder, A.: Explaining shipping company participation in voluntary vessel emission reduction programs, Transportation Research Part D: Transport and Environment, 61, 234–245, https://doi.org/10.1016/j.trd.2017.07.004, 2018.

Luoma, K., Virkkula, A., Aalto, P., Lehtipalo, K., Petäjä, T., and Kulmala, M.: Effects of different correction algorithms on absorption coefficient – a comparison of three optical absorption photometers at a boreal forest site, Atmospheric Measurement Techniques, 14, 6419–6441, https://doi.org/10.5194/amt-14-6419-2021, 2021.

MacGillivray, A., Li, Z., Hannay, D., Trounce, K., and Robinson, O.: Slowing deep-sea commercial vessels reduces underwater radiated noise, The Journal of the Acoustical Society of America, 146, 340–351, https://doi.org/10.1121/1.5116140, 2019.

MEPC, I.: 2021 Guidelines for Exhaust Gas Cleaning Systems, 2021.

Nunes, R. A., Alvim-Ferraz, M. C., Martins, F. G., Calderay-Cayetano, F., Durán-Grados, V., Moreno-Gutiérrez, J., Jalkanen, J. P., Hannuniemi, H., and Sousa, S. I.: Shipping emissions in the Iberian Peninsula and the impacts on air quality, Atmospheric Chemistry and Physics, 20, https://doi.org/10.5194/acp-20-9473-2020, 2020.

Orellano, P., Reynoso, J., Quaranta, N., Bardach, A., and Ciapponi, A.: Short-term exposure to particulate matter (PM10 and PM2.5), nitrogen dioxide (NO2), and ozone (O3) and all-cause and cause-specific mortality: Systematic review and meta-analysis, Environment International, 142, 105 876, https://doi.org/10.1016/J.ENVINT.2020.105876, 2020.

https://doi.org/10.5194/egusphere-2023-2823
Preprint. Discussion started: 12 February 2024

Parnell, K. E., Soomere, T., Zaggia, L., Rodin, A., Lorenzetti, G., Rapaglia, J., and Scarpa, G. M.: Ship-induced solitary Riemann waves of depression in Venice Lagoon, Physics Letters, Section A: General, Atomic and Solid State Physics, 379, 555–559, https://doi.org/10.1016/j.physleta.2014.12.004, 2015.

Petzold, A., Hasselbach, J., Lauer, P., Baumann, R., Franke, K., Gurk, C., Schlager, H., and Weingartner, E.: Experimental studies on particle emissions from cruising ship, their characteristic properties, transformation and atmospheric lifetime in the marine boundary layer, Atmospheric Chemistry and Physics, 8, 2387–2403, https://doi.org/10.5194/acp-8-2387-2008, 2008.

Petzold, A., Ogren, J. A., Fiebig, M., Laj, P., Li, S.-M., Baltensperger, U., Holzer-Popp, T., Kinne, S., Pappalardo, G., Sugimoto, N., Wehrli, C., Wiedensohler, A., and Zhang, X.-Y.: Recommendations for reporting "black carbon" measurements, Atmospheric Chemistry and Physics, 13, 8365–8379, https://doi.org/10.5194/acp-13-8365-2013, 2013.

Roo, S. D. and Troch, P.: Evaluation of the Effectiveness of a Living Shoreline in a Confined, Non-Tidal Waterway Subject to Heavy Shipping Traffic, River Research and Applications, 31, 1028–1039, https://doi.org/10.1002/RRA.2790, 2015.

Schlaerth, H., Ko, J., Sugrue, R., Preble, C., and Ban-Weiss, G.: Determining black carbon emissions and activity from in-use harbor craft in Southern California, Atmospheric Environment, 256, 118 382, https://doi.org/10.1016/J.ATMOSENV.2021.118382, 2021.

Seppälä, S. D., Kuula, J., Hyvärinen, A.-P., Saarikoski, S., Rönkkö, T., Keskinen, J., Jalkanen, J.-P., and Timonen, H.: Effects of marine fuel sulfur restrictions on particle number concentrations and size distributions in ship plumes in the Baltic Sea, Atmospheric Chemistry and Physics, 21, 3215–3234, https://doi.org/10.5194/acp-21-3215-2021, 2021.

Service, R. F.: Study Fingers Soot as a Major Player in Global Warming, Science, 319, 1745–1745, https://doi.org/10.1126/science.319.5871.1745, 2008.

Sinha, P., Hobbs, P. V., Yokelson, R. J., Christian, T. J., Kirchstetter, T. W., and Bruintjes, R.: Emissions of trace gases and particles from two ships in the southern Atlantic Ocean, Atmospheric Environment, 37, 2139–2148, https://doi.org/https://doi.org/10.1016/S1352-2310(03)00080-3, 2003.

Stumbo, S., Fox, K., Dvorak, F., and Elliot, L.: Prediction, measurement, and analysis of wake wash from marine vessels, Marine Technology and SNAME News, 36, 248–260, https://doi.org/10.5957/MT1.1999.36.4.248, 1999.

Tan, R., Psaraftis, H. N., and Wang, D. Z.: The speed limit debate: Optimal speed concepts revisited under a multi-fuel regime, Transportation Research Part D: Transport and Environment, 111, 103 445, https://doi.org/10.1016/J.TRD.2022.103445, 2022.

Townsin, R. L. and Kwon, Y. J.: Approximate formulae for the speed loss due to added resistance in wind and waves, RINA Transactions, 125, 1983.

Townsin, R. L. and Kwon, Y. J.: Estimating the Influence of Weather on Ship Performance, RINA Transactions, 135, 1993.

Viana, M., Rizza, V., Tobías, A., Carr, E., Corbett, J., Sofiev, M., Karanasiou, A., Buonanno, G., and Fann, N.: Estimated health impacts from maritime transport in the Mediterranean region and benefits from the use of cleaner fuels, Environment International, 138, 105 670, https://doi.org/10.1016/J.ENVINT.2020.105670, 2020.

Virkkula, A., Mäkelä, T., Hillamo, R., Yli-Tuomi, T., Hirsikko, A., Hämeri, K., and Koponen, I.: A simple procedure for correcting loading effects of aethalometer data, Journal of Air & Waste Management Association, 57, 1214–1222, https://doi.org/10.3155/1047-3289.57.10.1214, 2007.

Wang, L., Li, Y., Wan, Z., Yang, Z., Wang, T., Guan, K., and Fu, L.: Use of AIS data for performance evaluation of ship traffic with speed control, Ocean Engineering, 204, 107 259, https://doi.org/10.1016/J.OCEANENG.2020.107259, 2020.

Wang, X., Shen, Y., Lin, Y., Pan, J., Zhang, Y., Louie, K. K., Li, M., and Fu, Q.: Atmospheric pollution from ships and its impact on local air quality at a port site in Shanghai, Atmospheric Chemistry and Physics, 19, https://doi.org/10.5194/acp-19-6315-2019, 2019.

https://doi.org/10.5194/egusphere-2023-2823
Preprint. Discussion started: 12 February 2024

Wickham, H.: ggplot2, Springer New York, https://doi.org/10.1007/978-0-387-98141-3, 2009.

Woo, D. and Im, N.: Spatial Analysis of the Ship Gas Emission Inventory in the Port of Busan Using Bottom-Up Approach Based on AIS Data, Journal of Marine Science and Engineering, 9, 1457, https://doi.org/10.3390/jmse9121457, 2021.

Woo, D. and Im, N.: Estimation of the Efficiency of Vessel Speed Reduction to Mitigate Gas Emission in Busan Port Using the AIS Database, Journal of Marine Science and Engineering, 10, 435, https://doi.org/10.3390/jmse10030435, 2022.

Yau, P. S., Lee, S.-C., and Ho, K. F.: Speed Profiles for Improvement of Maritime Emission Estimation, Environmental Engineering Science, 29, 1076–1084, https://doi.org/10.1089/ees.2011.0399, 2012.

Zhang, C., Shi, Z., Zhao, J., Zhang, Y., Yu, Y., Mu, Y., Yao, X., Feng, L., Zhang, F., Chen, Y., Liu, X., Shi, J., and Gao, H.: Impact of air emissions from shipping on marine phytoplankton growth, Science of The Total Environment, 769, 145 488, https://doi.org/10.1016/J.SCITOTENV.2021.145488, 2021.